Phenotype Switching in Chemotaxis Aggregation Models Controls the Spontaneous Emergence of Large Densities

Path Tracking Control for Autonomous Driving Applications

Antonio Tota[1], Mauro Velardocchia[1] and Levent Güvenç[2]

[1] Politecnico di Torino, Torino 10123, Italy,
antonio.tota@polito.it,
WWW home page: http://www.polito.it/
[2] Ohio State University, Columbus (OH) 43210, USA,
guvenc.1@osu.edu,
WWW home page: mekar.osu.edu

Abstract. Autonomous or self-driving vehicles are becoming a consolidate reality that involves both industrial and academic fields also for its impact in social and governmental communities, well far from automotive engineering. The intent of the present paper is to design an automatic steering control for an autonomous vehicle equipped with steer-by-wire and drive-by-wire technologies. The steering action is calculated to let the vehicle follow a reference path which is stored in a Digital Map properly built to be available in real-time. A Proportional + Derivative (PD) control strategy is deigned based on the Parameter State Approach (PSA) and it is coupled with a Feedforward (FF) term for improving the path tracking control in cornering maneuvers. Some experimental results are shown to demonstrates the efficacy of the controller presented.

Keywords: Path Tracking control, Autonomous steering, Steer-by-wire experimental test

1 Introduction

'Autonomous driving' represents a generic term for identifying a non conventional vehicle that is able to drive in urban and/or highway scenarios without or with a partial human intervention. In order to provide a common terminology, in [1] are considered different levels of driving automation from *no automation* in 'level 0' to *full automation* in 'level 5'. The paper is focused on the analysis and the development of the control layer in the specific application of an automatic steering control for path tracking purposes. The path tracking control is a well-known topic in the robotic control field [2, 3]. Several experiments were carried out for automatic driving [4, 5] where the reference path is generally provided through inductive cables or magnetic markers, but new technologies about Global Positioning Systems (GPS) have incremented the position accuracy. Different feedback controllers have been designed for automated path tracking control and they can be generally divided into two separate categories.

The first category includes all methods based on simple geometrical relationships by exploiting the vehicle kinematic models (i.e. by approximating a zero

slip angle for the front and rear tires) described by the well-known Ackerman steering formula; One example is the *Pure Pursuit* algorithm whose objective is to calculate the the curvature of the arc that joints the vehicle position to desired position placed at a *look-ahead* distance on the reference path [6, 7].

The second category deals with all feedback controllers based on the simplified linear single-track model that takes into account a different slip angle for the front and rear axles and provides a second order yaw dynamics with damping and stiffness coefficients variable with vehicle speed; The Proportional Integral Derivative (PID) is the most used control logic adopted for steering angle evaluation: a PD structure on the lateral deviation error added to a P control on heading error is designed by [8] which proves that yaw angle error contribution further improves the tracking performance also confirmed by [9] where only the lateral position error is taken into account with evident worse results. The benefits introduced by a feedforward contribution which avoid the selection of high feedback control gain is shown by [10] thus also demonstrating its importance in terms of tradeoff between stability and tracking performances. In [11] a PIDD^2 controller is designed, according to the parameter state approach [12], for the path tracking problem related to an automated bus in order to be robust with respect to the variation of vehicle speed and mass in a specific range. The same state parameter approach is used for autonomous passenger vehicle by [13, 14]. A Linear Quadratic Regulator (LQR) is proposed by Nissan [9] that provides a comparison with a PD controller. Finally, other controller structures are designed with sliding mode [15], H_∞ [16] and model predictive strategy [17].

The paper is divided into seven sections by including the present introduction and the conclusion: section 2 shows the autonomous vehicle demonstrator; in section 3 the single-track model with steering dynamics is presented; section 4 gives few details about Digital map for reference path generation; section 5 in focused on path tracking control design which is finally implemented and experimentally verified in section 6.

2 Autonomous Demonstrator Vehicle

The vehicle demonstrator used for dynamics model validation and control calibration is a Ford Fusion hybrid which has been converted into an autonomous vehicle through the installation of steer-by-wire, throttle-by-wire and brake-by-wire Dataspeed interfaces and it is shown in Fig. 1. The Dataspeed modules are connected through CAN bus communication to a dSpace microautobox electronic unit for controlling the steering angle, the acceleration and brake action and for measuring the steering and gas/brake pedal positions. A range of several sensors are installed on-board vehicle (Delphi ESR radar, Velodyne VLP-16 Lidar, Mobileye camera and OXTS xNAV550 RTK GPS) in order to monitor the external environment. For the present activity, the differential GPS is the only sensor used for vehicle position localization as feedback input to the path tracking controller and it communicates with the microautobox via UDP protocol.

Fig. 1. Autonomous Vehicle Demonstrator at Automated Driving Lab in the Center for Automotive Reasearch of the Ohio State University

3 Vehicle Modeling and Experimental Validation

The present section is focused on the description of the vehicle linear single-track model and the steering dynamic equations, that will be experimentally validated through the vehicle demonstrator of Fig. 1.

3.1 Single-Track Model

The assumption for the single-track model (STM) are:

1. the vehicle is assumed as a rigid body with mass m and inertia moment J_z
2. vehicle speed V is constant
3. only two degree of freedom (yaw rate $r = \dot{\psi}$ and sideslip angle β) are considered
4. vehicle sisdeslip angle β, tires slip angles α_i and yaw rate acceleration $\dot{r}$ are considered small enough to consider the linear part of vehicle dynamics
5. small front wheel steering angles δ_w

The two degrees of freedom equations can be expressed as (see Fig. 2):

$$\begin{cases} mV(\dot{\beta} + r) & = F_y \\ J_z \dot{r} & = M_z \end{cases} \tag{1}$$

where F_y and M_z are the total lateral force and yaw moment expressed in vehicle reference frame:

$$\begin{cases} F_y & = \sum_{\forall i} F_{x_i} \sin(\delta_i) + \sum_{\forall i} F_{y_i} \cos(\delta_i) \approx \sum_{\forall i} F_{x_i} \delta_i + \sum_{\forall i} F_{y_i} \\ M_z & = \sum_{\forall i} F_{x_i} \sin(\delta_i) x_i + \sum_{\forall i} F_{y_i} \cos(\delta_i) x_i \approx \sum_{\forall i} F_{x_i} \delta_i x_i + \sum_{\forall i} F_{y_i} x_i \end{cases} \tag{2}$$

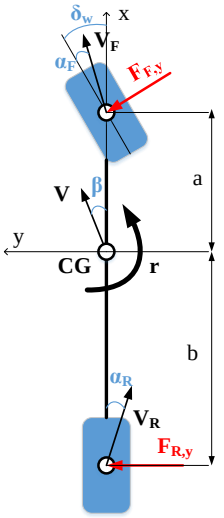

Fig. 2. Single-Track model general scheme

where F_{x_i}, F_{y_i} are force components on i_{th} axle and x_i, y_i are the coordinates of its center. In (2), drag forces and self-alignment yaw moments are neglected and trigonometric functions are linearized by considering low values of wheel steering angles δ_i. Tires lateral forces F_{y_i} depends on several variables such us tires slip angles, tires vertical forces, road contact friction coefficients and tires slip ratio. In order to have a linearized model, they can be evaluated as $F_{y_i} = C_i \alpha_i$ where C_i is the cornering stiffness of i_{th} axle and not of an individual wheel. Equivalent slip angles of front α_F and rear α_R axles can be evaluated from geometrical relations in wheels reference frame as reported in the following equations:

$$\begin{cases} \alpha_F &= \delta_F - \beta - \frac{a}{V} r \\ \alpha_R &= -\beta + \frac{b}{V} r \end{cases} \tag{3}$$

where a and b are respectively the front and rear vehicle semi-wheelbase. The final equation of linearized single-track vehicle model are:

$$\begin{cases} mV(\dot{\beta} + r) &= (-C_F - C_R)\beta + (-\frac{C_F a}{V} + \frac{C_R b}{V})r + C_F \delta_F \\ J_z \dot{r} &= (-C_F a + C_R b)\beta + (-\frac{C_F a^2}{V} - \frac{C_R b^2}{V})r + (C_F a)\delta_F \end{cases} \tag{4}$$

It is a system of two first order differential equations in terms of β and r with the steering angle δ_F as input for the system. Some of the single-track model parameters (m,J_z,a and b) are obtained through specific test rig measurements on the vehicle meanwhile the front C_F and rear C_R cornering stiffness values are assumed constant and proper tuned in order to get the best fit between model and experimental data. Ramp steer and Step steer maneuvers are executed on

a flat surface (no bank angle) and in high friction conditions for validating the single-track model. The ramp steer maneuver (gradually increase of steering angle at a constant vehicle speed of 30 km/h) is useful to observe the static lateral behavior of the vehicle in the whole range of lateral acceleration. The step steer maneuver is usually adopted for analyzing the transient vehicle behavior since it consists of an instantaneous constant steering action at a constant vehicle speed of 30 km/h. One comparison example between experimental data and single-track model output in terms of yaw rate, sideslip angle and lateral acceleration is reported in Fig. 3.

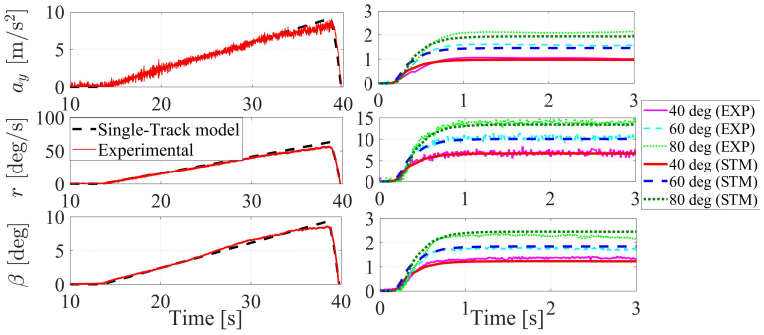

Fig. 3. Ramp and Step steer maneuver: sideslip angle β, yaw rate $r = d\psi/dt$ and lateral acceleration a_y from experimental test (EXP) and single-track model (STM)

3.2 Steering Dynamics

The steer-by-wire system consists of an electric motor directly connected to the steering column able to provide a desired angular position. A system identification analysis of steering actuation is carried out through a sweep frequency test (SFT) in order to plot its frequency response function (FRF) between the output signal δ_{Out} (measured steering angular position) and the desired steering command δ_{In}. The SFT consists of applying a sinusoidal steering command with a constant amplitude and variable frequency (linear time-variant):

$$\begin{cases} \delta_{In} & = \delta_0 \sin(2\pi f(t)t) \\ f(t) & = f_0 + \frac{f_T - f_0}{T} t \end{cases} \tag{5}$$

where $f_0 = 0.001\,Hz$ is the frequency at initial time t_0 and $f_T = 5\,Hz$ the frequency at time $T = 100\,s$. By using the System Identification Toolbox of Matlab®, different transfer function structures are taken into consideration and a comparison in terms of number of poles and zeros is shown in Fig. 4. A first order transfer function is not able to match magnitude neither phase lag of experimental FRF even with the adoption of one zero properly designed; a second

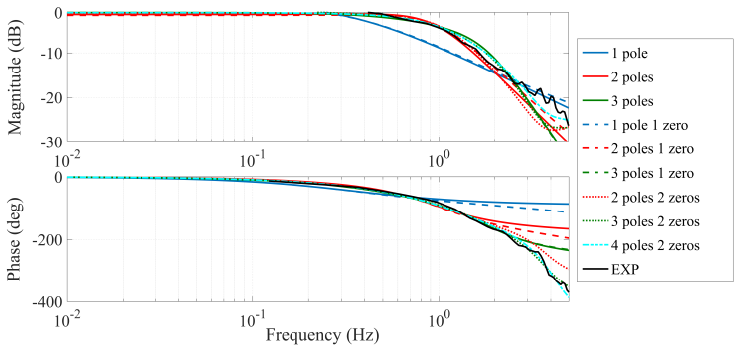

Fig. 4. System identification: comparison with experimental FRF at 90 deg against different transfer function structures

order transfer function can better describe system response up to a maximum frequency of 2 Hz and the introduction of 2 zeros improves the phase delay identification but with a negative influence on the magnitude for high frequency values. A 4^{th} order transfer function with 2 zeros is finally selected as a good linear model for describing the real system up to a maximum operating frequency condition of 5 Hz:

$$H(s) = \frac{\delta_{Out}}{\delta_{In}} = \frac{n_2 s^2 + n_1 s + n_0}{n_4 s^4 + n_3 s^3 + n_2 s^2 + n_1 s + n_0} \tag{6}$$

3.3 Lateral Deviation Equations

For the path tracking control design, the steering model must be extended including not only velocities (β and r) but also the vehicle heading and its lateral position with respect to the reference path. Fig. 5 shows shows an inertial coordinate frame x_0, y_0 and a vehicle body fixed coordinate frame x, y, which is rotated by the yaw angle ψ. The component of the vehicle speed V perpendicular to V_t is equal to the rate change of y_{CG}. The perpendicular component is expressed by $Vsin(\beta + \Delta\psi)$, where $\Delta\psi = \psi - \psi_t$ is the angle between the tangent to the path and the x axis of the vehicle. With the linearization $\sin(\beta + \Delta\psi) \approx \beta + \Delta\psi$, the lateral deviation in the center of gravity y_{CG} changes according to:

$$\dot{y}_{CG} = V(\beta + \Delta\psi) \tag{7}$$

The distance y at the so called *preview distance* l_s is here considered as controller input instead of y_{CG} since it constitutes a prediction variable thus enhancing the promptness of path tracking control strategy. The preview lateral deviation can be expressed as:

$$y = y_{CG} + l_s \sin(\Delta\psi) \approx y_{CG} + l_s \Delta\psi \tag{8}$$

changes both with $\dot{y}_{CG}$ and under the influence of vehicle yaw rate $r = \dot{\psi}$, and the rate change of the new displacement y is:

$$\dot{y} = V(\beta + \Delta\psi) + l_s \Delta\dot{\psi} = V(\beta + \Delta\psi) + l_s r - l_s \dot{\psi}_t \tag{9}$$

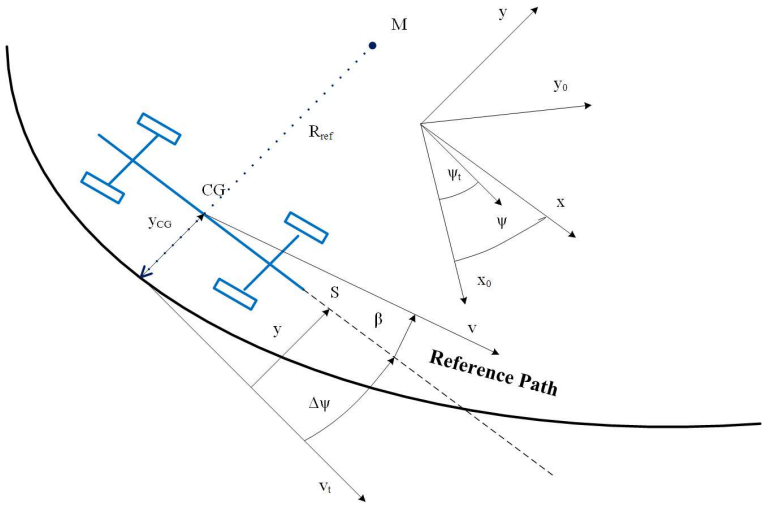

Fig. 5. Scheme representation of vehicle lateral deviation with respect reference path

where $\dot{\psi}_t = V/R_{ref} = V\rho_{ref}$ is the yaw rate of the path tangent in stationary circular cornering. Finally, the extended lateral deviation model can be obtained by combining (9) with the single-track and steering response equations (4) and (6). With the introduction of (9), the reference curvature ρ_{ref} appears as a second input to the system in addition to the steering angle δ_{In}.

4 Digital Map Generation

The reference path is converted offline into a Digital Map as explained in [14] and which consists of dividing the reference path into a predetermined number of segments and each of them is approximated by a third order parametric polynomial of the distance parameter γ:

$$\begin{cases} X_i(\gamma) = a_{Xi}\gamma^3 + b_{Xi}\gamma^2 + c_{Xi}\gamma + d_{Xi} \\ Y_i(\gamma) = a_{Yi}\gamma^3 + b_{Yi}\gamma^2 + c_{Yi}\gamma + d_{Yi} \end{cases} \tag{10}$$

where γ is the trajectory parameter and its value changes from 0 to 1 for the I segment, from 1 to 2 for the II segment and so on until the last segment. a_{Xi},b_{Xi},c_{Xi},d_{Xi} and a_{Yi},b_{Yi},c_{Yi},d_{Yi} are the polynomial coefficients of the X and Y components respectively of i_{th} segment. The determination of polynomial coefficients is obtained through a constrained least squares problem where the continuity of path, of the tangent to the path and its instantaneous curvature is preserved. Fig. 6 shows an example of the path segmentation and its comparison with respect the original set of data points. The digital map well describes the real data set with the advantage of using a considerably smaller amount of data whose quantity depends only on the number of segments chosen and no more linked to the number of original data points.

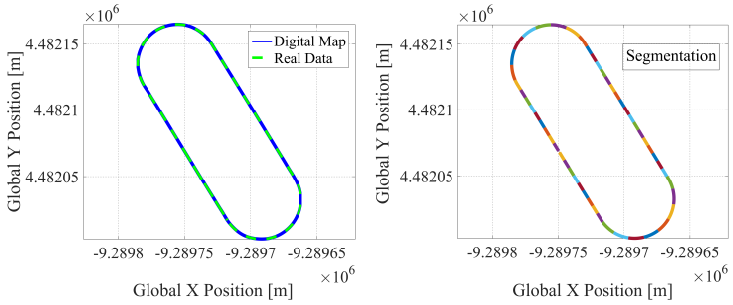

Fig. 6. Digital map creation: segmentation of real data (right) and comparison of digital map with real data (left)

5 Path Tracking Control

The present section aims to describe a PD+FF path tracking control for keeping the preview lateral deviation as small as possible even in presence of reference curvature changing ρ_{ref}.

5.1 PD Design with Parameter State Approach

Hurwitz and Gamma stability concepts are shown in [12] and its application to an automatic steering is reported in [14]. In the present section, the PSA approach is extended for the single-track model augmented with the steering dynamics equations. By applying the Laplace transformation to Eqs. (4), (6) and (9), the following transfer functions between preview lateral deviation and input steering angle is obtained:

$$\begin{aligned}\frac{y(s)}{\delta_{In}(s)} &= G(s) \\ &= \frac{(C_F J_z V^2 + l_s C_F a m V^2)s^2 + (C_F C_R V b l + l_s V C_F C_R l)s + V^2 C_F C_R l}{s^2 Den(s)} H(s)\end{aligned} \tag{11}$$

where $Den(s) = mV^2 J_z s^2 + (C_F V J_z + C_R V J_z + C_F a^2 m V + C_R b^2 m V)s + C_F C_R l^2 + m V^2 b C_R - m V^2 a C_F$. As controller structure, a PD logic is selected, $\frac{\delta_{In}(s)}{e(s)} = K_P + K_D s$ where $e(s) = y_{ref} - y$. The polynomial of the closed loop transfer function between the reference lateral deviation $y_{ref} = 0$ and the actual lateral deviation y can be expressed as a function of controller gains $p(s, K_P, K_D)$, by considering nominal vehicle parameters and a constant speed of $15km/h$. The Real Root (RRB), Infinite Root (IRB) and Complex Root Boundaries (CRB) are evaluated in the $K_P - K_D$ plane in Fig. 7 by constraining the s variable of $p(s, K_P, K_D)$ in the half-left plane for Hurwitz stability and in the D-stable region for Gamma stability. The RRB and CRB boundaries according

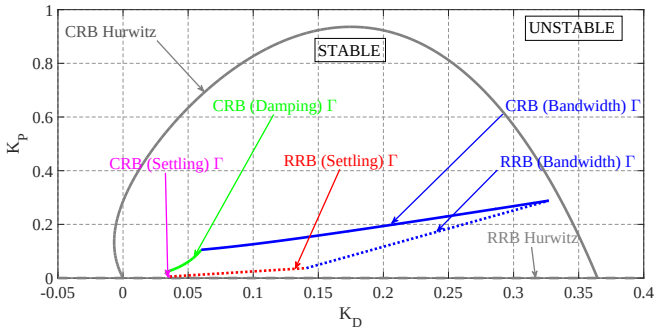

Fig. 7. Hurwitz and Gamma stability design criteria for lateral deviation control: boundaries and stability regions

to Hurwitz stability are marked with gray line thus separating the stable regions (left-half section of Argand-Gauss plane) from the unstable one: with this method a conservative selection of controller gains may be adopted if the task is only the close-loop system stability. In many controller design, the guarantee of stability is not sufficient for the specific application since more performances factor must be satisfied and the gamma stability concept can contribute to satisfy eigenvalues specifications in terms of settling time ($\sigma_0 = 0.3$), damping factor ($\alpha = 30\,deg$) and bandwidth ($R_b = 1.3$) selection; The most critical parameter is the bandwidth constraint since the steer-by-wire system has a cut-frequency almost equal to $1Hz$, meanwhile the other two requirements σ_0 and α can be selected with a greater margin. As shown in Fig. 7, Γ region is encapsulated in Hurwitz one since gamma stability adds more constraints on desired eigenvalues placement. Each pairs of K_P and K_D values inside the Γ region satisfies the lateral deviation control requirements.

5.2 Static Linear Feedforward Design

The preview lateral deviation is influenced by two input: the steering angle δ_{In} and the curvature of the reference path ρ_{ref}. The PD control logic has been designed by considering only the transfer function $G(s)$ between δ_{In} and y and it requires a further improvement to take into account the curvature ρ_{ref}. In the present section the Static Linear Feedforward (FF) method is introduced and designed by considering that ρ_{ref} can be easily obtained by the Digital Map, since segments of reference path are approximated by a third order polynomial and the value of curvature is expressed by:

$$\rho_{ref}(p) = \frac{X'_p Y''_p - Y'_p X''_p}{\left(X'_p X'_p + Y'_p Y'_p\right)^{3/2}} \tag{12}$$

where X'_p, Y'_p are the first derivative and X''_p, Y''_p the second derivative respectively of X_p and Y_p with respect γ_i. The FF is an open-loop control designed in

order to provide a value of δ_{FF} based on the current value of $\rho_{ref}(p)$ and this can be obtaining by inverting the steady-state relation between steering angle and vehicle curvature expressed by single-track model:

$$\delta_{FF} = (L + KV^2)\rho_{ref}(p) \tag{13}$$

where $K = \frac{m}{L}(\frac{b}{C_F} - \frac{a}{C_R})$ represents the vehicle understeer gradient and $L = a+b$ its wheelbase.

6 Experimental Results

The PD logic designed with the parameter state approach is added to the FF contribution to provide the steering angle as input to the autonomous vehicle shown in Fig. 1 which is requested to follow the reference path of Fig. 6. The vehicle speed is kept constant at $15km/h$ by using a Proportional Integral (PI) cruise control experimentally tuned and not discussed in the present paper. The path tracking is executed in both autonomous mode (PD and PD+FF) and manual mode by a common driver; the results are shown in Fig. 8. It is visible

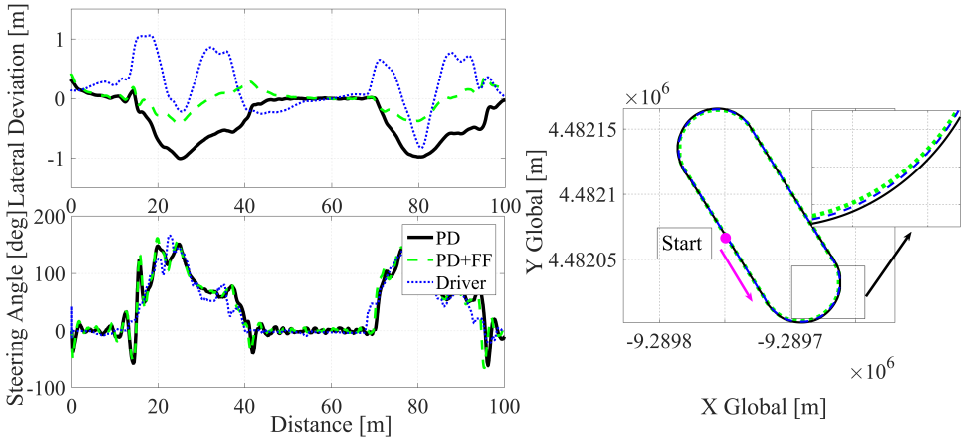

Fig. 8. Lateral deviation y, steering angle δ_{Out} and Global coordinates during autonomous path tracking with PD and PD+FF strategies at constant speed of $15km/h$

that the PD+FF control provides better results if compared with the PD logic and with the driver behavior: the FF contribution provides a steering additional contribution based on the calculation of reference curvature ρ_{ref} that can modify the PD control performances when applied alone, in particular during the cornering part of the path.

7 Conclusion

The present paper shows a real application of autonomous steering logic for path tracking control. A linear-single track model experimentally validated is used for vehicle modeling and a system identification method is applied for steering dynamics. The simple linear model is able to describe vehicle lateral behavior for low values of lateral accelaration. A PD + FF control strategy is designed by involving steering dynamics and reference path curvature influence and it has been implemented on a vehicle demonstrator equipped with steer-by-wire technologies. An experimental maneuver is executed on the proving ground for proving the efficacy of PD and PD+FF controller and for comparing their benefits with respect to a manual driving. Experimental results proves that even a so simple controller structure is able to provide a good tracking performance (max 50 cm of error with respect reference path) in nominal road conditions (flat surface with high friction coefficient).

References

1. S. O.-R. A. V. S. Committee *et al.*, "Taxonomy and definitions for terms related to on-road motor vehicle automated driving systems," 2014.
2. L. Lapierre, R. Zapata, and P. Lepinay, "Combined path-following and obstacle avoidance control of a wheeled robot," *The International Journal of Robotics Research*, vol. 26, no. 4, pp. 361–375, 2007.
3. D. Verscheure, B. Demeulenaere, J. Swevers, J. De Schutter, and M. Diehl, "Time-optimal path tracking for robots: A convex optimization approach," *IEEE Transactions on Automatic Control*, vol. 54, no. 10, pp. 2318–2327, 2009.
4. R. Oshima, E. Kikuchi, M. Kimura, and S. Matsumoto, "Control system for automobile driving," in *Proceedings of the Tokyo 1FAC Symposium*, 1965, pp. 347–357.
5. R. E. Fenton and R. J. Mayhan, "Automated highway studies at the ohio state university-an overview," *IEEE transactions on Vehicular Technology*, vol. 40, no. 1, pp. 100–113, 1991.
6. R. C. Coulter, "Implementation of the pure pursuit path tracking algorithm," DTIC Document, Tech. Rep., 1992.
7. J. M. Snider *et al.*, "Automatic steering methods for autonomous automobile path tracking," *Robotics Institute, Pittsburgh, PA, Tech. Rep. CMU-RITR-09-08*, 2009.
8. S. Tsugawa, "An overview on control algorithms for automated highway systems," in *Intelligent Transportation Systems, 1999. Proceedings. 1999 IEEE/IEEJ/JSAI International Conference on.* IEEE, 1999, pp. 234–239.
9. H. Mouri and H. Furusho, "Automatic path tracking using linear quadratic control theory," in *Intelligent Transportation System, 1997. ITSC'97., IEEE Conference on.* IEEE, 1997, pp. 948–953.
10. H. Inoue, H. Mouri, H. Sato, A. Asaoka, and S. Ueda, "Technologies of nissan's ahs test vehicle," in *3rd ITS World Congress*, 1996.
11. J. Ackermann, J. Guldner, W. Sienel, R. Steinhauser, and V. I. Utkin, "Linear and nonlinear controller design for robust automatic steering," *IEEE Transactions on Control Systems Technology*, vol. 3, no. 1, pp. 132–143, 1995.
12. J. Ackermann, *Robust control: the parameter space approach.* Springer Science & Business Media, 2012.

13. J. Guldner, W. Sienel, H.-S. Tan, J. Ackermann, S. Patwardhan, and T. Bunte, "Robust automatic steering control for look-down reference systems with front and rear sensors," *IEEE transactions on control systems technology*, vol. 7, no. 1, pp. 2–11, 1999.
14. M. T. Emirler, H. Wang, B. A. Güvenç, and L. Güvenç, "Automated robust path following control based on calculation of lateral deviation and yaw angle error," in *ASME 2015 Dynamic Systems and Control Conference*. American Society of Mechanical Engineers, 2015, pp. V003T50A009–V003T50A009.
15. T. Hiraoka, O. Nishihara, and H. Kumamoto, "Automatic path-tracking controller of a four-wheel steering vehicle," *Vehicle System Dynamics*, vol. 47, no. 10, pp. 1205–1227, 2009.
16. R. T. O'Brien, P. A. Iglesias, and T. J. Urban, "Vehicle lateral control for automated highway systems," *IEEE Transactions on Control Systems Technology*, vol. 4, no. 3, pp. 266–273, 1996.
17. P. Falcone, F. Borrelli, J. Asgari, H. E. Tseng, and D. Hrovat, "Predictive active steering control for autonomous vehicle systems," *IEEE Transactions on control systems technology*, vol. 15, no. 3, pp. 566–580, 2007.